Vertical variation of oxygen isotope in Bay of Bengal and its relationships with water masses

S. Sengupta,[1] Anant Parekh,[1] S. Chakraborty,[1] K. Ravi Kumar,[1] and T. Bose[1]

Received 23 March 2013; revised 29 October 2013; accepted 30 October 2013; published 3 December 2013.

[1] We present here, for the first time, comprehensive depth specific (near surface to 1800 m) oxygen isotope (δ^{18}O) data set of 175 water samples collected from 22 different locations in the Bay of Bengal (BoB) during July–August 2009 and December–January 2012–2013. The study is aimed to constrain the water mass parameters using oxygen isotope and salinity. Four water masses are identified on the basis of temperature-salinity relationship: (a) Bay of Bengal Water (BoBW; 0–50 m), (b) Mixed Zone (MZ; 60–120 m), (c) Indonesian Throughflow (ITF; 200–500 m), and (d) Indian Ocean Deep Water (IDW; 600–1800 m). Our study shows: (1) δ^{18}O-salinity correlation (slope = 0.15 ± 0.01; intercept = −4.58 ± 0.24; r^2 = 0.89; n = 54) for the BoBW is found to be consistent with surface BoB water reported earlier, (2) relatively lower correlation (r^2 = 0.24; n = 47) in underlying mixed zone suggesting mixing of various water masses, (3) significant linear correlation between δ^{18}O and salinity in IDW (r^2 = 0.70) indicating depleted less saline water from southern hemisphere spread up to 18°N, and (4) vertical profiles at various sampling locations showing a continuous enrichment of δ^{18}O (0.6–0.8‰) within top 60–100 m irrespective of their proximity to coastline. In conjunction with a sharp decrease in Δ^{14}C data below the same depth zone (60–100 m) as reported earlier, we suggest the δ^{18}O value reaches to its acme at a zone of mixing between younger BoBW and relatively older ITF. This preliminary study indicates oxygen isotope and salinity together can be used to identify different water masses in the BoB.

Citation: Sengupta, S., A. Parekh, S. Chakraborty, K. Ravi Kumar, and T. Bose (2013), Vertical variation of oxygen isotope in Bay of Bengal and its relationships with water masses, *J. Geophys. Res. Oceans*, *118*, 6411–6424, doi:10.1002/2013JC008973.

1. Introduction

[2] The Indian Ocean as a whole and the Bay of Bengal (BoB) in particular, provide a good laboratory for the study of paleoceanographic and paleoclimatic reconstructions and processes [*Sarkar et al*., 1990; *Burton and Vance*, 2000; *Pierson-Wickmann et al*., 2001; *Ahmad et al*., 2005]. Studies are essential for the understanding of ocean circulation, hydrological cycle, and ocean transport within a dynamic freshwater flux environment. The unique geographical setting of the Indian Ocean with northern boundaries being landmass and seasonal reversals of winds and currents creates a dynamic ocean environment (Figure 1). One tool used to study such dynamics is oxygen isotope (δ^{18}O) together with salinity and temperature. Such studies have been limiting due to the lack of extensive sampling.

[3] The available δ^{18}O data from northern Indian Ocean (in general) and BoB (in specific) are mainly confined to surface water (mostly up to a depth of 50 m) [*Delaygue et al*., 2001; *Somayajulu et al*., 2002; *Singh et al*., 2010; *Achyuthan et al*., 2013]. Most of the earlier studies established a specific correlation between salinity and δ^{18}O which could suitably be used for interpretation of paleoclimate data from various planktonic foraminifers [*Cullen*, 1981; *Duplessy*, 1982; *Sarkar et al*., 1990; *Rashid et al*., 2011]. Salinity and δ^{18}O of surface water were used to understand the mixing of various surface water masses in northern and southern Indian Ocean [*Srivastava et al*., 2007; *Tiwari et al*., 2013]. However, compared to ocean surface, oxygen isotope data from deeper BoB water are rarely reported. Limited deeper BoB water δ^{18}O data (at 50 m) reported so far indicate no visible change of slope and intercept values from their surface counterpart [*Singh et al*., 2010]. Due to paucity of depth specific δ^{18}O data, it was practically impossible to study whether the slope and intercept change systematically with depth.

[4] Depth specific studies of oxygen isotope could be useful to understand the formation of near surface stratification and vertical mixing in BoB which has a significant impact on monsoonal activity. The stratification in BoB occurs due to high precipitation, low evaporation, and large amount of freshwater discharge by five of the world's 50 largest rivers [*Gopalkrishna et al*., 2002; *Vinayachandran et al*., 2002]. In this region the mixed layer is shallower [*Shenoi et al*., 2002] and barrier layer is deeper

Additional supporting information may be found in the online version of this article.

[1]Indian Institute of Tropical Meteorology, Pune, India.

Corresponding author: S. Sengupta, Indian Institute of Tropical Meteorology, Pune, Maharashtra 411008, India. (saikat@tropmet.res.in)

2169-9275/13/10.1002/2013JC008973

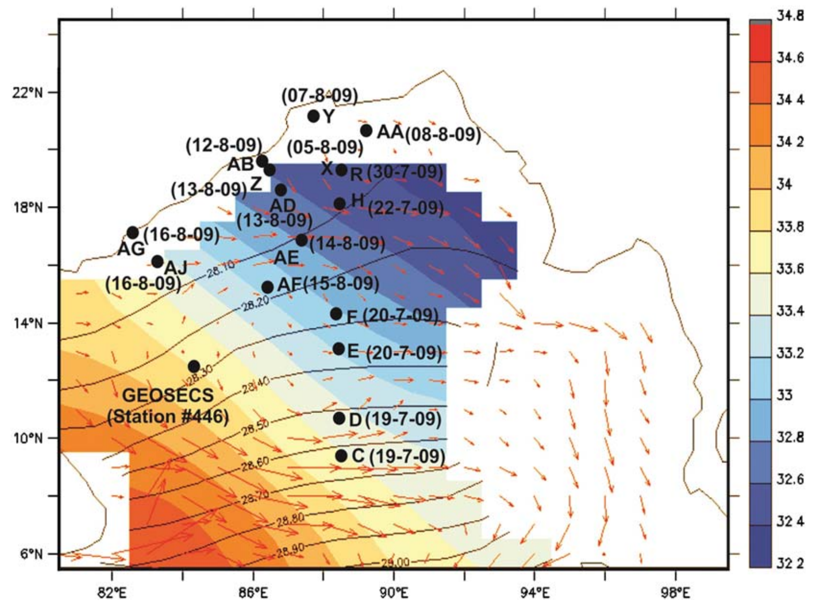

Figure 1. Sample location map in BoB. Locations are marked as black filled circle and sampling dates are also mentioned in parenthesis adjacent to sample location. One GEOSECS (Station 446) location is also marked. Surface salinity in PSU (shaded), temperature in °C (contour) and horizontal surface current distribution from GODAS in cm/s for the BoB during July–August 2009.

[*Girishkumar et al*., 2011]. In the presence of a shallow mixed layer, the air-sea fluxes affect intraseasonal sea surface temperature (SST) fluctuations and air-sea interaction which finally impact on monsoon activity via monsoon intraseasonal oscillation [*Sengupta et al*., 2002; *Parekh et al*., 2004; *Klingaman et al*., 2008; *Achuthavarier and Krishnamurthy*, 2011]. The formation and thickness of both mixed layer and barrier layer are controlled by vertical mixing between surface freshwater and deep saline water [*Vinayachandran et al*., 2002]. However, the processes associated with the vertical mixing have not been studied extensively due to lack of observations [*Sengupta et al*., 2006; *Vinayachandran et al*., 2012]. Especially, ambiguity still exists on how deep freshwater reaches and which physical processes determine its extent of reach [*Sengupta et al*., 2006]. Salinity and δ^{18}O profiles together would help to understand the physical processes and circulation in deeper water as they have been used elsewhere [*Fairbanks*, 1982; *Frew et al*., 1995, 2000; *Meredith et al*., 1999, 2013; *Yi et al*., 2012].

[5] The usefulness of salinity-δ^{18}O correlations in surface and deeper water has been discussed in many previous studies [e.g., *Adkins et al*., 2002; *Abrahamsen et al*., 2009]. The slope and intercept of salinity-δ^{18}O linear regression for coastal ocean are generally found to be sensitive to the amount and isotopic composition of discharged freshwater [*Bigg and Rohling*, 2000, Figure 1]. In open surface ocean, where runoff component (RO) is minimal, the corresponding slope is controlled by precipitation (P), evaporation (E), upwelling, advection, and diffusion [*Benway and Mix*, 2004]. Both parameters (i.e., salinity and δ^{18}O) increase due to net evaporation ($E > P + RO$) and decrease due to net freshwater input ($P + RO > E$) at the surface. The slopes and intercepts are higher in Arctic, Antarctic, and subtropical ocean and lower in tropical and equatorial ocean [*Legrande and Schimdt*, 2006]. Based on drifted ice-sheets and their subsequent melting to isotopically depleted water, surface Arctic Ocean shows relatively large slope (0.48 ± 0.007‰/PSU) and intercept (-16.82 ± 0.234‰) values [*Pfirman et al*., 2004]. Similar high slopes and intercepts were also observed in north Atlantic, south Atlantic, north Pacific, Labrador Sea, and other subtropical oceans [*Fairbanks*, 1982; *Ostlund et al*., 1987]. On the other hand, tropical Atlantic and Indian Oceans, with no significant contribution of melt water, are characterized by small slopes (0.15 ± 0.008‰/PSU and 0.16 ± 0.004‰/PSU, respectively) and intercepts (-4.61 ± 0.297‰ and -5.31 ± 0.135‰), respectively [*Ostlund et al*., 1987; *Delaygue et al*., 2001; *Singh et al*., 2010]. Interestingly, depending on local advection and upwelling, surface and deeper ocean water may show contrasting values of slopes and intercepts. For example, deeper Arctic Ocean has considerably higher slope (0.84 ± 0.005‰/PSU) and intercept (-29.16 ± 0.162‰) compared to its surface counterpart (0.48 ± 0.007‰/PSU) and (-16.82 ± 0.234‰), respectively [*Pfirman et al*., 2004]. This all suggests that vertical variation of isotope values and their correlation with corresponding salinity data are highly sensitive to various physical processes.

[6] Toward this, we present here, for the first time, depth controlled δ^{18}O data set (up to 1800 m) from 22 locations in the northern BoB. An attempt has been made to explain the vertical variation of isotope values with respect to physical oceanographic processes and variation of water masses. This study presents unique approach to study BoB processes using isotope, current analysis, and ARGO observations.

2. BoB Water Column Structure

[7] A brief knowledge of water column structure (up to 2000 m) in BoB is prerequisite to understand the oxygen

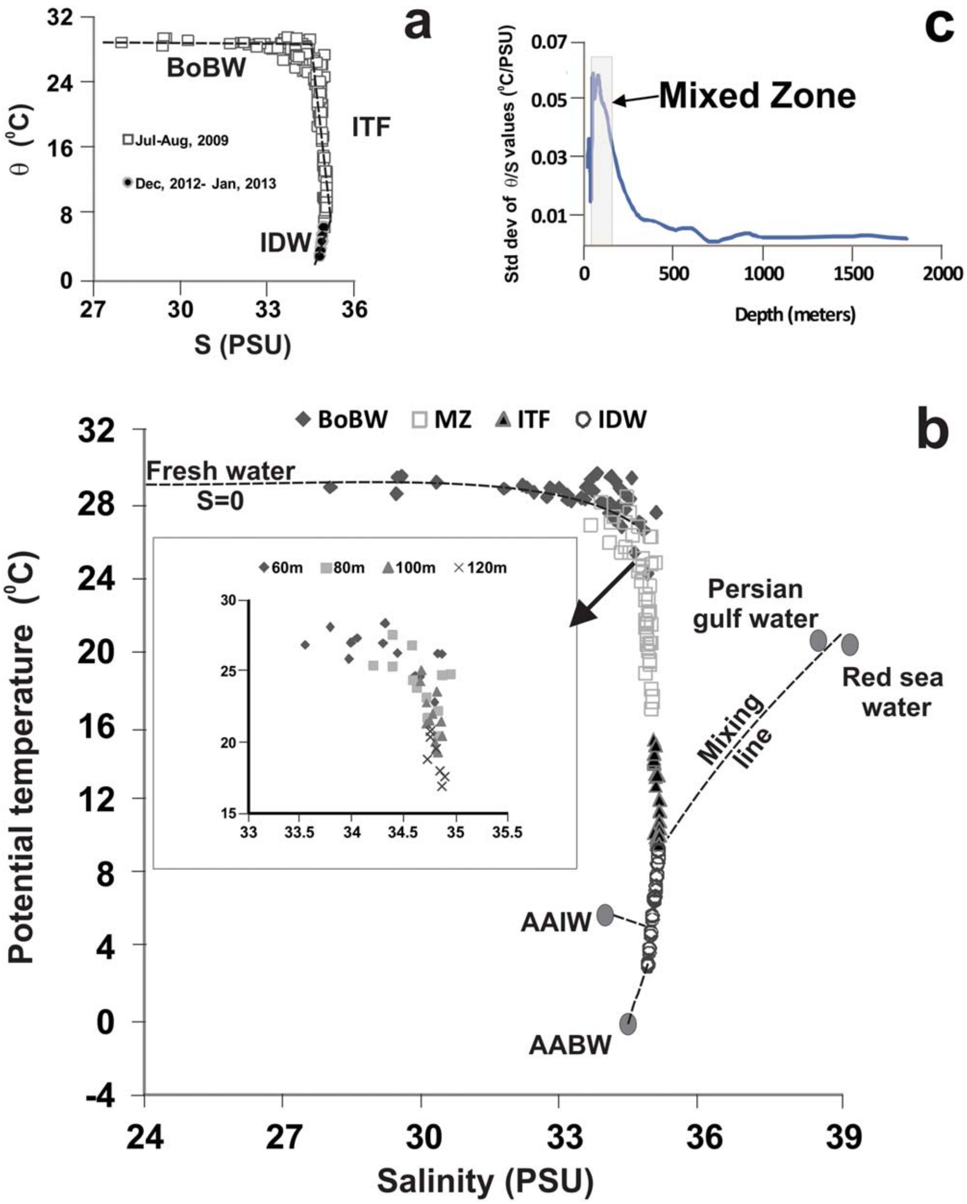

Figure 2. Potential temperature-salinity (θ-S) plot of the study area (a) all samples collected during July–August 2009 (open squares) and December 2012 to January 2013 (solid circles). Black dashed line indicates conventional θ-S plot and water mass classification in BoB after Tomczak et al. [2003]. (b) θ-S plot of water mass classification for total data set. Source water masses are shown as black solid circles. AABW = Antarctic Bottom Water; AAIW = Antarctic intermediate water; θ-S variation at various depths in mixed zone is shown in inset. (c) Depth specific standard deviation of θ/S values. Mixed zone is marked as gray area.

isotope profiles. Based on potential temperature-salinity (θ-S) correlations, three different water masses are identified in BoB (Figure 2a, *Murty et al*., 1992; *Tomczak and Godfrey*, 2003]. Within the top 80–100 m, the existence of BoB Water mass (BoBW) is demarcated by a sharp increase in salinity from ~28 to ~34.5 PSU accompanied by a small decrease in temperature (~1°C). From 100 to 500 m, existence of Australasian Mediterranean Water (AAMW) masses, a tropical water mass derived from Pacific Ocean Central Water formed during transit through the Indonesian Seas, is identified by a sharp decrease in temperature (28–8°C) and marginal increase in salinity by ~0.25 PSU. AAMW is often referred to as "Indonesian throughflow (ITF)" in literature [*Potemara*, 2005; *Nyadjoro et al*., 2010]. Intrusion of Red Sea and Persian Gulf water can also produce departure from θ-S curves near the isopycnal surface at $\sigma_t = 27.2$ and influence ITF water mass [*Kumar and Li*, 1996]. The demarcation between ITF and its lower adjacent water mass, Indian Ocean Deep Water (IDW) is gradational. A small decrease in salinity (by 0.3–0.4 PSU) is observed in IDW. IDW is considered as a northward advected front of Antarctic Bottom Water

(AABW) [*Clowes and Deacon*, 1935, Figure 2b]. Due to very sluggish circulation, ITF and IDW waters are considerably older than BoBW [*Dutta and Bhusan*, 2012]. On the other hand, top 30–40 m of BoBW, show strong seasonality in θ-S properties [*Prasad*, 2004]. The influx of freshwater (in the form of precipitation and river runoff) produces a thin mixed layer in the uppermost part of BoBW during Indian Summer Monsoon (ISM; June–September) [*Sengupta et al*., 2006]. Depending on net freshwater flux (P + RO − E), the thickness of mixed layer may vary from 30 to 10 m in a single location within summer monsoon [*Vinayachandran et al*., 2002]. A 30–40 m thick barrier layer exists below mixed layer and above thermocline [*Bhat et al*., 2001; *Vinayachandran et al*., 2002; *Thadathil et al*., 2007; *Agarwal et al*., 2012]. The sharp density contrast across barrier layer inhibits vertical mixing across this layer. Mixed layer and barrier layer together with a part of thermocline constitute BoBW [*Tomczak and Godfrey*, 2003].

[8] East Indian Coastal current is the dominant surface current in BoB during ISM which is drifted by southwesterly monsoonal wind. Discharged freshwater is distributed in eastern BoB by Ekman transport [*Shetye et al*., 1996; *Schott and McCreary*, 2001; *Shankar et al*., 2002; *Durand et al*., 2009]. Apart from these surface currents, a warm (27–23°C) and saline (35–35.2 PSU) water mass is advected northeastward at 50–100 m up to 14°N [*Murty et al*., 1993]. Intense vertical mixing is inferred at the zones of salinity fronts in the depth limits of 40–100 m and also at deeper depths (>2200 m) and elsewhere lateral mixing is predominant [*Murty et al*., 1992]. All these processes and sources of different water masses make BoB column structure very unique than any other Bay of global ocean.

3. Data Collection and Methodology

3.1. Sample/Data Collection

[9] The Continental Tropical Convergent Zone (CTCZ) program was conducted under the Indian Climate Research Program (ICRP). The detail science plan is available at http://www.imd.gov.in/SciencePlanofFDPs/CTCZ. Under the CTCZ, oceanic observations were taken on board ocean research vessel Sagar Kanya. The cruise (SK-261) was conducted during July–August 2009. The sample locations are shown in Figure 1 with surface salinity, temperature from ARGO observation, and current information from Global Ocean Data Assimilation System (GODAS) for the months July and August 2009. Water samples were collected at 15 locations from near surface to 500 m depth (supporting information Table S1 and Figure 1). Samples were also collected up to a depth of 1000 m from four locations AD, AE, AF, and AJ (supporting information Table S1). However, in shallower coastal BoB region (location Y, AB, and AG), collection of samples were possible only up to 100 m, 80 m, and 40 m depth, respectively. As limited samples were collected at 1000 m or deeper ocean during summer monsoon 2009, we studied the region again in December 2012 to January 2013 on board ORV Sagar Nidhi (SN-70) and collected samples (from 1000 to 1800 m) from six locations A-1, B-1, C-1, D-1, E-1, and F-1 (supporting information Table S1). All samples were stored in 100 ml doubly capped pesticide grade plastic bottles to avoid evaporation. Except for near surface samples (<10 m), temperature and conductivity of other samples were measured by Conductivity-Temperature-Depth (CTD) instrument manufactured by Idronaut with analytical accuracy of 0.001°C and 0.0001 Sm s^{-1}, respectively, and scan frequency of 40 Hz [*Rao et al*., 2011]. CTD profiler was calibrated against standard conductivity solution before the cruise. Salinity and density values were derived from temperature and conductivity using standard UNESCO equation of state [*Fofonoff and Millard*, 1984]. Salinity and temperature of near surface water (<10 m) was measured on board by Thermo-salinograph (TSG) with an external precision of 0.01%. Data from TSG were compared to that from CTD temperature and salinity for the upper ocean and they were found consistent with each other. Potential temperature is estimated following the equation of *Fofonoff and Millard* [1984].

3.2. Sample Analysis

[10] Water samples were equilibrated with CO_2 at 32°C in a gas bench and cleaned gases were measured (in duplicates) in a Thermo Scientific Delta V Plus mass spectrometer for δ^{18}O composition in the Stable Isotope Laboratory of the Indian Institute of Tropical Meteorology, Pune, India. The system was calibrated by analyzing International Atomic Energy Agency (IAEA) primary reference materials Vienna Standard Light Antarctic Precipitation (VSLAP), Vienna Greenland Ice Sheet Precipitation (VGISP), and Vienna Standard Mean Ocean Water (VSMOW). Analytical precision was monitored by running internal water standard NARM (prepared at Physical Research Laboratory, Ahmedabad from Narmada river water: δ^{18}O with respect to VSMOW = −3.45‰) with each set of samples. Long-term performance of NARM was routinely monitored by another secondary standard IITM-B (prepared at Indian Institute of Tropical Meteorology, Pune from normal reverse osmosis water and calibrated by three primary IAEA standards mentioned above). The difference between NARM and IITM-B, routinely measured, is 1.59 ± 0.04‰ (1σ) since the inception of stable isotope laboratory in 2009. 1σ error mentioned above is considered as the long-term precision of our measurement. All isotopic data are reported in ‰ (per mil) with respect to VSMOW.

3.3. Current Analysis and ARGO Observations

[11] To understand the role of various physical processes in depth specific variation of δ^{18}O, National Center for Environment Prediction (NCEP)'s GODAS based on the Geophysical Fluid Dynamics Laboratory, Modular ocean Model version 4p0 (MOM4p0) with a three-dimensional variational (3DVAR) data assimilation scheme is used [*Ravichandran et al*., 2011]. The GODAS is one of the state of the art systems providing all the three components of currents (zonal, meridional, and vertical) at various depths. The system is used to understand the role of advection in regulation of δ^{18}O with depth. Systematic assessment of GODAS for the tropical Indian Ocean is carried out by *Ravichandran et al*. [2013]. They compared GODAS temperature vertical structure with the Research Moored Array for African-Asian-Australian Monsoon Analysis and Prediction (RAMA) buoys and surface

temperature fields with Reynolds SST and similarly surface current with the Ocean Surface Current Analysis Realtime (OSCAR) and subsurface current with the RAMA buoys. They carried out the comparison exercise for the period of 2004–2009 and found with RAMA for the depth of 50–100 m, temperature root-mean-square error (RMSE) is $<0.8°C$ and below 100 m it is $<0.2°C$ and correlation is about 0.8 in the first 300 m. Comparison between GODAS and OSCAR surface currents shows that RMSEs for the eastern and western BoB are about 0.1 m/s and 0.2 m/s, respectively. Comparison with the current from RAMA buoys indicate RMSEs are about 0.4 m/s and about 0.3 m/s for the depth zones 30 to 100 m and further deeper to 300 m, respectively. The correlation coefficient is about 0.6. Separate comparison is also carried out for the north BoB current of GODAS and RAMA buoys and found that for the surface current RMSE is 0.2 m/s. Thus, GODAS currents are reasonably good and state of the art source of currents in the case of BoB. Besides, gridded (1° × 1°) ARGO surface and subsurface temperature and salinity observations are used to reveal the details of salinity and temperature structure during the study period in the BoB [*Agarwal et al*., 2012; *Udaya Bhaskar et al*., 2007].

4. Results and Discussion

4.1. Classification of Water Mass

[12] θ-S plots of the samples are shown in Figure 2. The summer and winter samples show nearly similar θ-S properties around 1000 m depth (Figure 2a). This supports that water below this depth is too old to show any seasonality in physical properties. Hence, physical and isotopic attributes of summer and winter samples from 1000 to 1800 m can be clubbed together for discussion of their depth specific variation. In addition to the three major water masses discussed earlier, a 60–70 m thick mixed zone is identified at the boundary of BoBW and ITF (Figure 2b). The mixed zone is characterized by considerably large spatial variations in salinity (33.70–35.00 PSU) and temperature (23–27°C). *Murty et al*. [1992] observed similar spatial variation of salinity nearly in the same depth zone (50–100 m) and explained those changes as being due to north-eastward propagating saline water plume from the Arabian Sea (AS). Though the salinity variation below 100 m across BoB is not well documented (Figure 2b, inset), a large salinity variation between a coastal profile Y and an open BoB profile C is observed at 60 and 80 m (supporting information Table S1). Moreover, depth specific standard deviation of θ/S values shows (Figure 2c) two prominent peaks at the depths of 60 and 120 m indicating the depth zone of maximum variation of θ/S values. Therefore, on the basis of θ/S variation in present study and comparison with literature, the following four water masses are identified—(a) BoBW (depth: surface to 50 m; salinity: 24.97–34.96 PSU; temperature: 24.23–29.66°C), (b) mixed zone (MZ; depth: 60–120 m; salinity: 34.37–34.87 PSU; temperature: 16.95–28.3°C), (c) ITF (depth: 200–500 m; salinity: 34.92–35.01 PSU; temperature: 9.64–15.26°C), and (d) IDW (depth: 600–1800 m; salinity: 34.78–35.01 PSU; temperature: 3.12–9.37°C). Isotope property of each water mass will be subsequently discussed in the following sections.

4.2. Spatial Variation of $\delta^{18}O$ in Various Water Masses

4.2.1. Isotope Signature of BoBW

[13] Salinity, temperature, and $\delta^{18}O$ data of all samples are given in supporting information Table S1. Salinity and $\delta^{18}O$ relationships for various water masses are shown in Figure 3 and summary of correlation parameters are given in Table 1. BoBW shows significant correlation between salinity and $\delta^{18}O$ values ($r^2 = 0.89$; $n = 54$; Figure 3a). Interestingly, the slope ($s = 0.15 \pm 0.01‰$/PSU) and the intercept ($i = -4.58 \pm 0.24‰$) of the regression line obtained in this study are close to corresponding values ($s = 0.21 \pm 0.02‰$/PSU) and ($i = -6.9 \pm 0.7‰$) observed by *Singh et al*. [2010] for September–October 2002. In a recent study, *Achyuthan et al*. [2013] analyzed 194 samples collected from various locations in northern BoB and obtained similar slope ($0.14 \pm 0.01‰$/PSU) and intercept ($-4.7 \pm 0.04‰$) irrespective of the sampling locations though they showed large latitudinal variation (~0.8‰) of $\delta^{18}O$ and salinity (~8 PSU) similar to our observation. This indicates similar physical processes control salinity and $\delta^{18}O$ distribution in the top 50 m. Supporting information Table S1 further shows spatial variation of $\delta^{18}O$ being maximum within top 10 m (1.28‰ at surface and 0.93‰ at 10 m). The spatial variation gradually decreases to 0.36‰ at 50 m. A corresponding variation in salinity (Figure 2b) and significant correlation between $\delta^{18}O$ and salinity indicate considerable vertical mixing between surface freshwater and deep saline water. To understand whether this lateral variation of $\delta^{18}O$ is related to the advection of any depleted water plume, horizontal distribution of $\delta^{18}O$, and salinity (data from Argo observations) for various depth intervals (10, 50, 100, and 500 m) have been examined. Salinity, $\delta^{18}O$, and current directions at these depths for July and August 2009 are shown in Figures 4a–4d and 4e–4h, respectively. Figure 4a shows a significant isotopic depletion occurs toward north, northeast, and east at 10 m which can be attributed to proportionate dilution by freshwater discharges from north and eastern rivers of the Indian subcontinent. This is also supported by very strong positive gradient of salinity in southwest direction (Figure 4a) and eastward surface currents over this region (Figure 4e). The salinity distribution in top few meters of BoB, on the other hand, strongly depends on net freshwater flux (E-P). Figure 5a presents evaporation minus precipitation over the BoB for the study period. The figure shows that the northern BoB has negative freshwater flux (16–20 mm/day) and southern west BoB has positive freshwater flux. These numbers are in agreement with *Rao and Sivakumar* [2003], who reported that in the BoB north of 8°N, sea surface salinity falls from 32.5 to 31.5 PSU during July and August and this is mainly due to precipitation of 35 cm/month, river runoff of 10 cm/month and evaporation of 10 cm/month. *Rao and Sivakumar* [2003] also reported that Ganges, Brahmaputra, and Irrawaddy release 4×10^4 m^3/s, 6×10^4 m^3/s, and 2×10^4 m^3/s, respectively, water mass into the BoB during July and August. Thus eastern BoB freshening is partly due to precipitation and partly due to river runoff. Apart from net freshwater flux, salinity and $\delta^{18}O$ distribution of surface BoB water is also controlled by surface currents which are, in turn, connected to

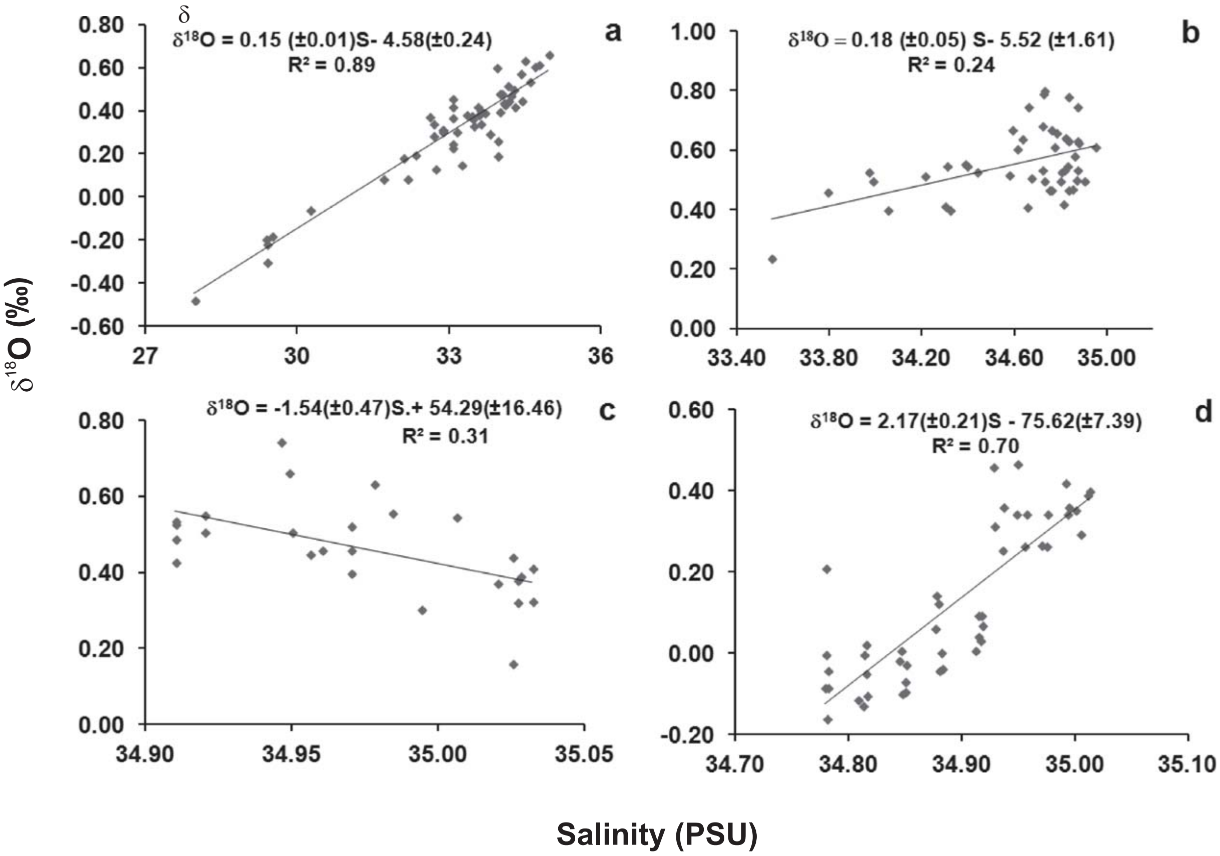

Figure 3. δ^{18}O-Salinity scatter plots for various water masses—(a) BoBW, (b) MZ, (c) ITF, and (d) IDW. Equations of regression line and correlation coefficients (R^2) at >99% significance level are mentioned in respective figures and summarized in Table 1.

monsoonal wind direction. Figure 5b shows surface wind speed (shaded) and direction (arrow) over the BoB for the study period (July–August 2009). Stronger wind of 9–11 m/s is observed in the central north BoB, while rest of the BoB is under wind speed of 6–8 m/s and the direction of the wind is south westerly over the basin. This southwesterly wind is responsible for the dominant south easterly Ekman transport (Figure 4e) in the BoB. This surface current advects freshwater toward the eastern BoB. Surface layer vertical motion is downward while the strongest downward motion is at 17°N zonal strip and at 10°N and 90°E (Figure 4e). Spatial variation of δ^{18}O at surface BoB in accordance with monsoonal wind direction has recently been documented by *Achyuthan et al*. [2013]. A significant isotopic depletion occurs toward east at the depth of 50 m that is accompanied by a corresponding change in salinity in latitude of 15°N (Figure 4b). In BoB surface, salinity is mainly dependent on the distribution of freshwater through ocean currents [*Shetye et al*., 1996]. From the current analysis, it is found that Ekman drift associated to south westerly monsoon winds (Figure 5b) push surface water toward the east (Figure 4f), which accumulates freshwater in eastern BoB and enhance vertical mixing with deeper water. Figures 4e and 4f indicate that downwelling is dominant both at the surface as well as at 50 m in the south of 18°N. Horizontal surface current is eastward in the entire study region, while at 50 m current is eastward in the north of 18°N, between 17°N and 13°N it is southward and south of 13°N it is northward. This circulation pattern leads to subsurface freshening in the eastern BoB. This drifted freshwater also moves southward all along the eastern coast of BoB [*Shankar et al*., 2002; *Vinayachandran et al*., 1999, 2002]. First 50 m stratification is quantified by energy required for mixing [*Shenoi et al*., 2002; *Agarwal et al*.,

Table 1. Regression Statistics of δ^{18}O-Salinity Correlations in Four Water Masses

Water Mass	Slope (‰/PSU)	Standard Error (‰/PSU)	Intercept (‰)	Standard Error (‰)	R^2	Standard Error	Number of Observations	Significance Level (%)
BoBW	0.15	0.01	−4.58	0.24	0.89	0.08	54	>99
MZ	0.18	0.05	−5.52	1.61	0.24	0.1	47	>99
ITF	−1.54	0.47	54.29	16.46	0.31	0.1	26	>99
IDW	2.17	0.21	−75.62	7.39	0.7	0.11	48	>99

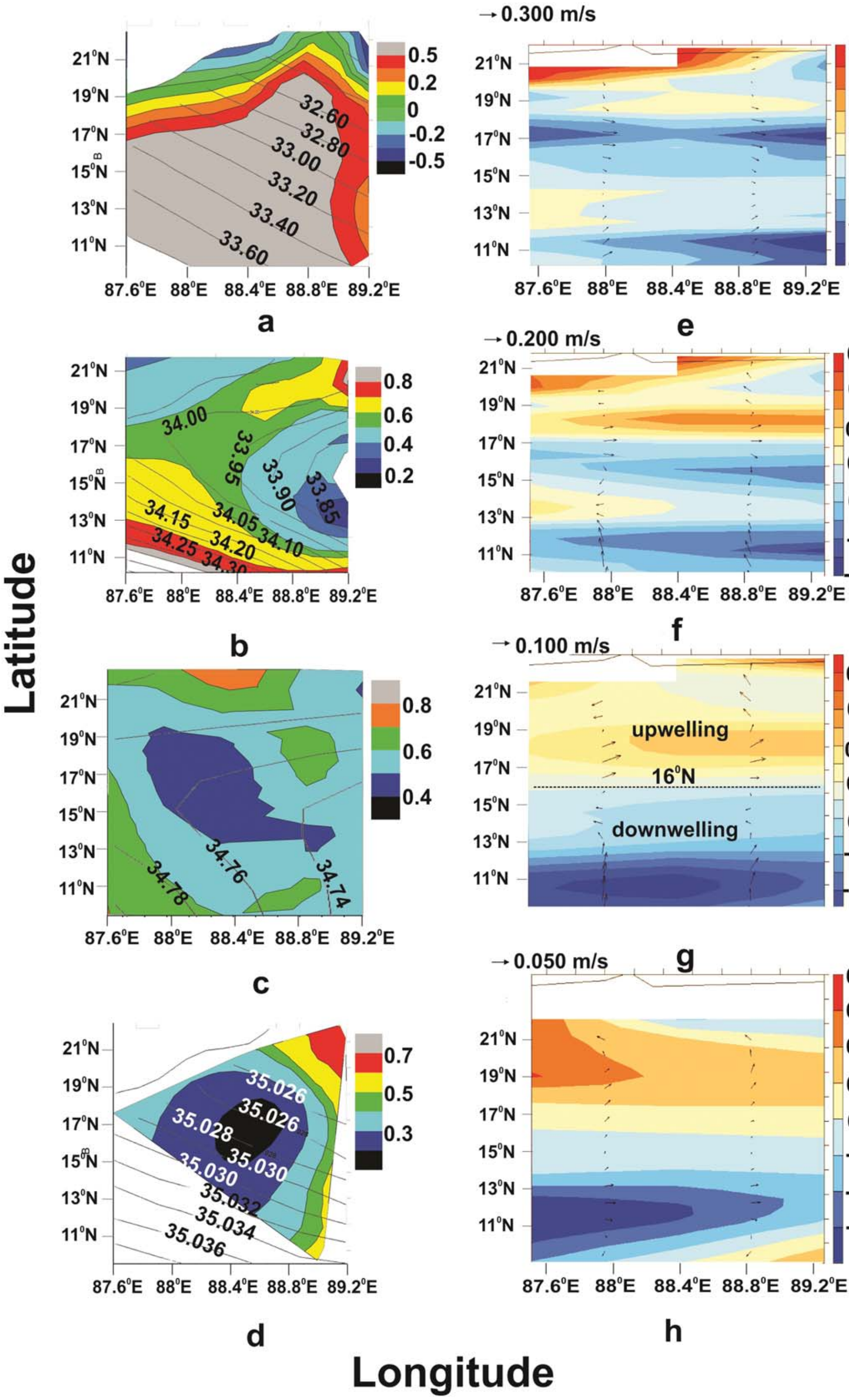

Figure 4. Salinity in PSU (contour) and $\delta^{18}O$ (shaded) in ‰ at (a) 10 m, (b) 50 m, (c) 100 m, and (d) 500 m. Vertical currents (shaded) in $\times 10^{-5}$ m/s and horizontal current direction and magnitude (m/s, arrows) at corresponding depths are in Figures 4e–4h.

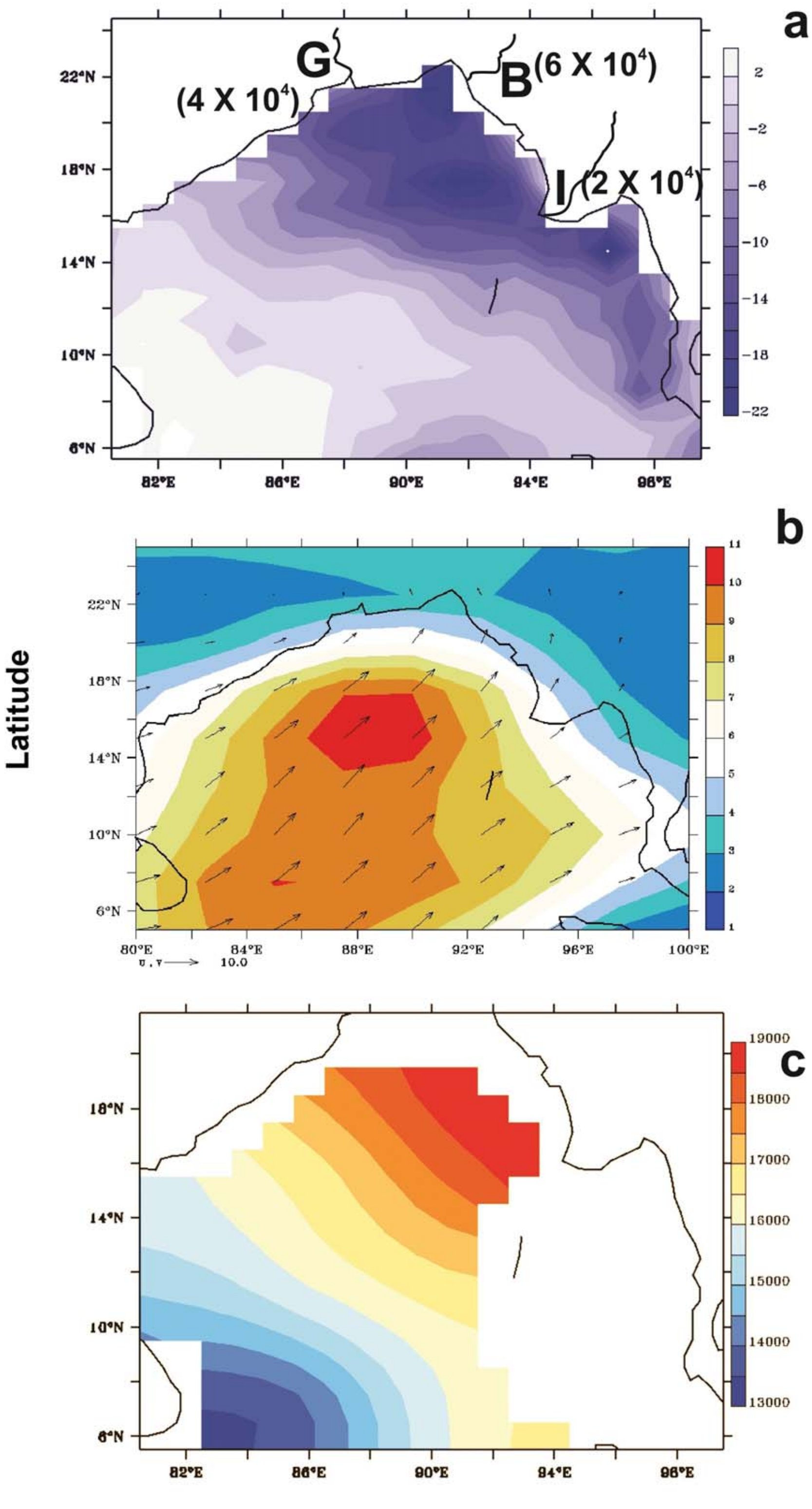

Figure 5. Spatial distribution of (a) freshwater flux (mm/day), (b) wind speed shaded (m/s) and direction (arrowed), and (c) ERM (J/m^2) over the study area during July–August 2009. Discharge rate (m^3/s) of three major rivers Ganges (G), Brahmaputra (B), and Irrawaddy (I) are also shown in parenthesis in Figure 5a.

2012]. Energy required for mixing (ERM) is estimated using the following relation and its horizontal distribution is shown in Figure 5c:

$$ERM = \frac{1}{8}(\rho_b - \rho_s)gh^2 \quad (1)$$

where ρ_s is density of surface layer water and ρ_b is density of 50 m layer water, g is acceleration due to gravity (9.8 m/s^2), and h is depth (50 m).

[14] It is found that within the top 50 m, stratification (Figure 5c) follows the distribution pattern of surface freshwater flux (Figure 5a). The southwestern BoB region is less stratified while the northeastern BoB is relatively more stratified with an ERM of about 18,000 J/m^2. The stratification in the northern BoB, as observed in ERM data, is resulted from high influx of river water and precipitation. Notably, July–August is the peak period of the SW monsoon over the subcontinent. Figure 4b shows the δ^{18}O enriched water mass in the north east of study area (north of 19°N and 88–90°E). Figures 4e and 4f reveal that it is due to strong coastal upwelling by southwesterly wind resulting in strong upward motion (0.6–0.8 × 10^{-5} m/s) of high saline water from below 50 m. Another enriched δ^{18}O water mass is in the southwest region, which is due to high saline water mass from the AS and southern Indian Ocean.

4.2.2. Isotope Signature of MZ

[15] Although slope (0.18 ± 0.05‰/PSU) and intercept (−5.52 ± 1.61‰) of regression line in MZ are very close to those of BoBW, δ^{18}O and salinity show significantly lower correlation in mixed zone (r^2 = 0.24, n = 47; Figure 3b and Table 1). Salinity and δ^{18}O distribution at 100 m show an eastward depletion (of maximum 0.4‰) in isotope values (Figure 4c). Notably, both salinity and δ^{18}O decrease near 16°N. A similar low salinity patch along 16°N was also identified by *Murty et al*. [1992]. While the prevailing wind (directed toward northeast; Figure 5b) aids the flows in the central BoB, the freshwater influenced thermohaline flow dominates the northeastern BoB (Figure 4g). Different vertical current direction across 16°N is documented in Figure 4g. All this possibly suggests different water masses mixing across the latitude and thus explains the lower correlation of δ^{18}O and salinity compared to that in a well-mixed water mass BoBW. Notably, very few δ^{18}O data from AS in that depth zone (60–120 m) are currently available [*Ostlund et al*., 1987]. Twenty-nine samples collected from various locations in south eastern AS at the depth of 50 m (marginally above MZ of our study area) show high mean δ^{18}O values [0.97 ± 0.43‰; *Singh et al*., 2010]. This suggests that higher δ^{18}O at 100 m in the southern part of our study area is a signature of mixing of isotopically enriched AS water from south and comparatively depleted water from north.

4.2.3. Isotope Signature of ITF

[16] Although no significant spatial variation of salinity (34.91–35.03) was observed, a large change in δ^{18}O (0.16–0.75‰) was visible in ITF zone (Figure 3c). A gradual enrichment of δ^{18}O toward north of the study area is observed at 500 m (Figure 4d). Currents show a sluggish flow from southwest to the study area (Figure 4h). It probably indicates an isotopically depleted front that might have been transported to the study area from southwest. Similar to MZ, δ^{18}O data are rarely available for the adjacent southeastern AS at this depth. This limits us to understand the extension of depleted front to the south. Nearest to our study area (10.10°N; 52.75°E), one δ^{18}O value (0.33‰) reported by *Epstein and Mayeda* [1953] suggested that the depleted front might not reach up to that location. However, due to our limited data set for that depth zone and insufficient data set in southeast AS, it is not possible to explain, at present, how this depleted water front migrated northeastward without any significant change in salinity. Another possible explanation for this significant spatial variation of isotope values at 500 m may be isopycnal mixing which has been discussed in detail later (see section 4.3).

4.2.4. Isotope Signature of IDW

[17] Similar to BoBW, IDW also shows considerable correlation between salinity and δ^{18}O (r^2 = 0.70; n = 48; Table 1). However, the slope (2.17 ± 0.21‰/PSU) and intercept (−75.62 ± 7.39‰) of IDW are higher than BoBW (Figure 3d). Although salinity range for this zone is slightly lower than that of its upper adjacent water mass (ITF), salinity-δ^{18}O correlation of these two layers are contrastingly different. Concurrent reduction of salinity and isotopic ratio most probably indicates occurrence of AABW in this depth zone even at the latitude of 18°N. Although oxygen isotopic signature of AABW in IDW was never reported earlier from BoB, similar high slope (~3‰/PSU) and intercept (−110‰) of δ^{18}O-salinity correlation was reported earlier from many locations between southern Indian Ocean and Antarctica [*Meredith et al*., 1999] and bottom water in Elizabeth trough at Antarctica [*Frew et al*., 1995]. It is important to note that though, based on water mass properties, AABW should exist between 2000 and 3800 m depth, but in Indian Ocean, the boundary between IDW and AABW is gradational [*Tomczak and Godfrey*, 2003]. Notably, based on some chemical tracers, i.e., dissolved nitrate, phosphate, and silica, *van Aken et al*. [2004] identified a fraction of North Atlantic Bottom Water (NABW) in IDW at southwestern Indian Ocean. However, a much lower slope ($\Delta\delta^{18}O/\Delta S$ = 0.61‰/PSU) of North Atlantic mix line, as reported by *Frew et al*. [2000] suggests NABW front is possibly not migrated to northeastern part of Indian Ocean and further to BoB.

4.3. Vertical Variation of δ^{18}O

[18] Vertical variation of δ^{18}O along with salinity, temperature, and density are shown in Figure 6. Figures 6a and 6b show depth profiles along two sections in coastal BoB and Figure 6c shows that along a section in open BoB. A gradual but systematic enrichment of δ^{18}O with depth (shallower than 100 m) is found in all the profiles. In the SE coastal section AB-Z-AD (Figure 6a), the enrichment is of 0.71‰ (location AD; −0.08‰ to 0.63‰) to 0.86‰ (location Z; from −0.18‰ to 0.68‰). In all three locations, peak δ^{18}O values are obtained at the same depth (80 m). Similar depth specific trend is also seen in another eastern coastal section Y-X-R (Figure 6b). However, the peak isotope values are found at different depths (100 m for Y and R; 60 m for X). The magnitude of maximum variation (from surface to 60 m/100 m) in all locations of Y-X-R profile (1.51‰, 1.00‰, and 1.12‰ for Y, R, and X, respectively) is considerably higher than that of AB-Z-AD. These

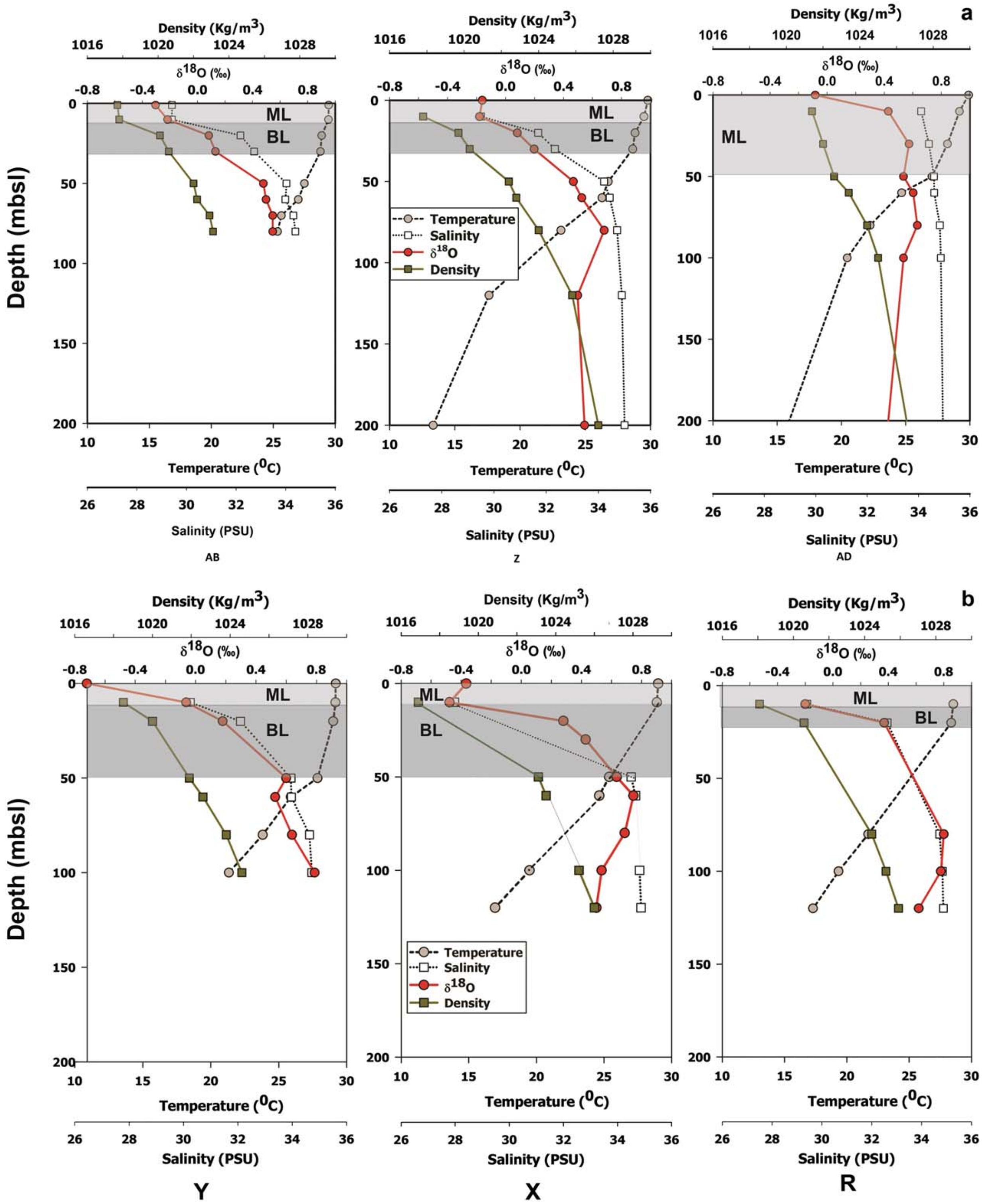

Figure 6. Vertical variation of $\delta^{18}O$ (in ‰), salinity (PSU), temperature (°C), and density (kg/m^3) of shallow subsurface (up to 200 m) at three sections—(a) south eastern coastal bay (AB-Z-AD), (b) eastern coastal bay (Y-X-R), and (c) open bay (C-D-F). Mixed (ML) and barrier layer (BL) are marked in each section. See Figure 1 for sample locations and sections.

profiles are from the north BoB and very close to the river mouth of Ganges and Brahmaputra, which are discharging huge freshwater to BoB. Notably, $\delta^{18}O$ peak for all six locations are very close (mean $\delta^{18}O = 0.65$; $1\sigma = \pm 0.11$) although surface water $\delta^{18}O$ are markedly different (−0.72‰, −0.37‰, and −0.2‰, respectively, for Y, X, and R and −0.18‰, −0.30‰, and −0.08‰ for Z, AB, and AD, respectively). This is consistent with the surface

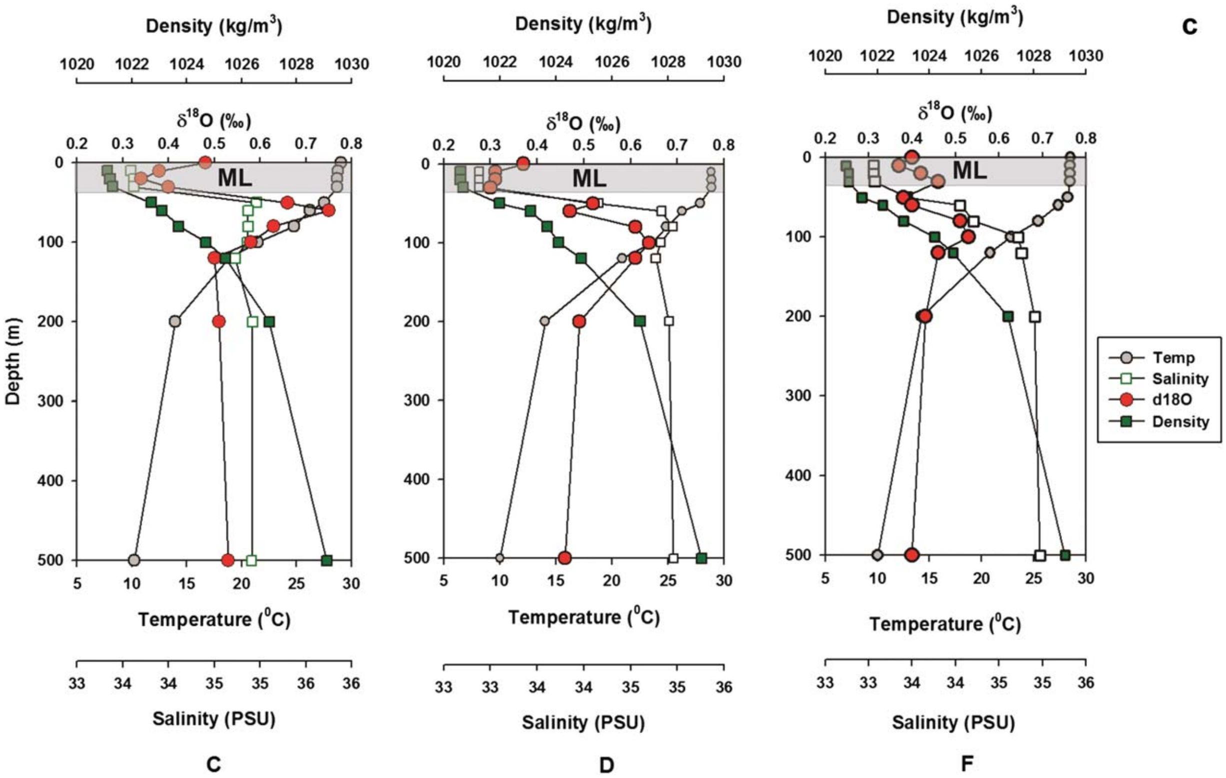

Figure 6. (Continued)

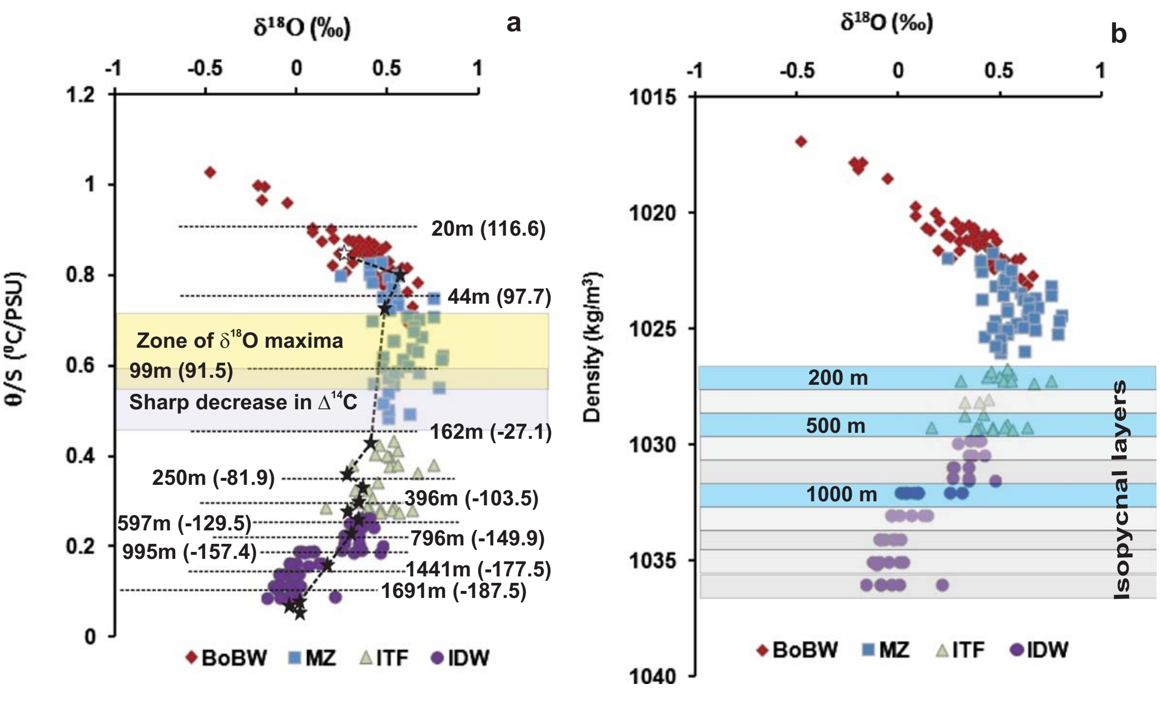

Figure 7. (a) θ/S versus δ^{18}O plot for various water masses. Legend is given below. Solid black stars represent data for the only GEOSECS location (Station #446) in the study area [*Ostlund et al.*, 1987]. Black dotted horizontal lines indicate the depth intervals at which Δ^{14}C (‰) data are available from GEOSECS study [*Ostlund et al.*, 1987]. Numbers in parenthesis next to the depth values denote concentration of Δ^{14}C at that level. Violet transparent field marks a sharp decrease of Δ^{14}C values from 99 to 162 m. Yellow field indicates zone of δ^{18}O maxima. For the GEOSECS location, please see Figure 1. Black dotted line joining the stars represents the trend of δ^{18}O in GEOSECS location. (b) Density (kg/m^3) versus δ^{18}O (‰) plot for various water masses. Isopycnal layers are shown in ITF and IDW. Isopycnal layers (transparent blue) at 200, 500, and 1000 m show some variation of δ^{18}O.

salinity distribution in the BoB (Figure 1) and E-P features (Figure 5a). More depleted surface BoB δ^{18}O values in eastern coastal profile (Y-X-R) indicate higher amount of freshwater by various eastern Indian rivers during this period [*Sengupta et al.*, 2006]. Similar to the two coastal sections, the open BoB section (C-D-F) also shows a gradual enrichment of δ^{18}O with depth up to 60–100 m (Figure 6c). Mean peak δ^{18}O (at 60–100 m) in open BoB is very close ($\mu = 0.66‰$; $1\sigma = \pm 0.06‰$) to that of coastal BoB section. Surface water δ^{18}O values in open BoB (0.48‰, 0.38‰, and 0.40‰ for C, D, and F, respectively) are more enriched than that of their coastal counterparts. All this suggests that isotopic depletion in surface water due to river discharges is more pronounced in the coastal bay than the open bay (Figure 5a). A gradual enrichment of 0.3‰ in δ^{18}O of surface water from coastal to open BoB has also been reported earlier [*Delaygue et al.*, 2001; *Singh et al.*, 2010]. Additionally, our study shows a δ^{18}O maxima exists at the depth of 80 ($\pm$20) m in both coastal and open BoB. Notably, depth of δ^{18}O peak apparently is not correlated with mixed layer and barrier layer depth. Mixed layer and barrier layer exist within top 20 m and between 20 and 40 m, respectively, in the coastal BoB (Figures 6a and 6b). In open BoB, mixed layer is thicker (40 m) and barrier layer is thinner (Figure 6c). This indicates that mixing between low density freshwater and higher density deep saline water controls the density distribution of top 40 m in north coastal BoB. Though vertical variation of δ^{18}O values within top 40–50 m mostly support the mixing phenomena mentioned above, peak δ^{18}O (80 $\pm$ 20 m) are found within the thermocline region, below the barrier layer (Figure 6c). Recent studies show proliferation of zooplankton and a corresponding oxygen minima zone below the barrier layer at BoB [*Naqvi et al.*, 1994; *Sarma*, 2002]. δ^{18}O values of dissolved oxygen obtained from this oxygen minima zone are generally 10–15‰ enriched than the threshold values of dissolved oxygen [*Nakayama et al.*, 2008]. However, abundance of $H_2{}^{18}O$ and $H_2{}^{16}O$ in BoB water are many times higher than those in dissolved oxygen. Therefore, no significant change in isotope values of BoB water is expected due to isotope exchange with that species mentioned earlier. We, therefore, consider the depth of peak δ^{18}O as the maximum depth of vertical mixing and further consider the intermediate δ^{18}O values within the top 80–100 m signify a two component physical mixing between peak and most depleted surface BoB values. Figure 7a shows isotope values reach acme within MZ and the high values persist in ITF but gradually fall in IDW. Depth specific Δ^{14}C values of BoB water collected from one location at BoB in 1976 [*Ostlund et al.*, 1987] and at many locations in BoB, reported recently by *Dutta and Bhushan* [2012] indicate a sharp decrease (from 92‰ to -27‰ in GEOSEC location 446) in Δ^{14}C below 80–100 m (Figure 7). The rate of decrease of Δ^{14}C concentration ($\delta\Delta^{14}C/\delta h$) above and below of MZ/ITF boundary is 1.88‰/m and 1.60‰/m, respectively. Although no GEOSECS Δ^{14}C data is currently available at 120 m (lower boundary of MZ in the present study), the available radiocarbon profile clearly shows presence of old water below 160 m and relatively younger water above 100 m. Therefore, considering the uncertainty due to paucity of Δ^{14}C data between 100 and 160 m, we suggest the oxygen isotope peak at 80 ($\pm$20) m demarcates the boundary of two different water masses of different ages (younger BoBW and older ITF). Closer inspection of vertical profiles (Figure 6) shows salinity slowly increases to 100–120 m. But no more significant increase in salinity is observed in ITF. Salinity further decreases marginally in IDW, which is accompanied by a simultaneous decrease in δ^{18}O (Figures 3d and 7). Therefore, vertical distribution of δ^{18}O in BoB mostly follows the salinity distribution, and peak δ^{18}O zone is characterized by the zone of vertical mixing between two water masses (BoBW and ITF). The relation between δ^{18}O and density is shown in Figure 7b. This analysis reveals that below the 100 m with respect to isopycnal level, δ^{18}O spread is about 0.3–0.4‰. Highest spread is found at 200–500 m and the spread gradually decreases below 500 m. The spread is very small at 1035 isopycnal level. This spatial variation of δ^{18}O between the 150 to about 500 m lies in the subthermocline region. The region is known for isopycnal mixing [*Hirst and Cai*, 1994]. Hence, the spatial variation of isotope values can be related to mixing within isopycnal layers. However, more observations on δ^{18}O and eddies at that depth zone are required to confirm the role of isopycnal mixing on isotope values.

5. Conclusion and Implication

[19] Based on δ^{18}O, salinity, temperature, and density records of 175 water samples collected from northern BoB and deep BoB water current analysis, our study identifies:

[20] 1. Four water masses—(a) BoB Water (BoBW), depth: surface to 50 m, (b) Mixed Zone (MZ), depth: 60–120 m, (c) Indonesian Throughflow (ITF) depth: 200–500 m, and (d) Indian Ocean Deep Water (IDW) depth: 600–1800 m.

[21] Slope and intercept of δ^{18}O-salinity regression line and correlation coefficient of those two parameters for BoBW (top 50 m) are very close to that of surface water reported earlier. This indicates that mixing of BoBW extends more than 50 m. Spatial variation of δ^{18}O at 50 m, in accordance with corresponding variation of salinity and current data indicate strong downward movement of depleted freshwater front.

[22] 2. Large spatial variability of δ^{18}O in mixed zone possibly indicates mixing of various water masses during Indian Summer Monsoon.

[23] 3. Regression parameters of δ^{18}O-salinity relationship of IDW and AABW indicate deeper water of BoB is possibly derived from Antarctic Bottom Water though earlier work indicates a large fraction of IDW is derived from North Atlantic Bottom water.

[24] 4. Vertical variation of δ^{18}O profiles show a maxima at the depth of 80 $\pm$ 20 m indicating a considerable vertical mixing of two water masses, viz, BoBW and ITF. θ/S ratio of this study and Δ^{14}C profile from other studies also support the mixing of two water masses close to the zone of δ^{18}O maxima.

[25] Hence, this study, for the first time, in BoB suggests that the vertical profiling of sea water δ^{18}O can be used to identify water masses and associated physical processes especially to study the three-dimensional distribution of water masses in the BoB.

[26] Moreover, the subsurface δ^{18}O peak and the δ^{18}O-salinity relationship could be used to model the paleo-BoB

circulation. This may be employed by suitably varying the slope and intercept encompassing the high and low monsoon regime. Proxy records indicate that summer monsoon was significantly intensified (weakened) about 10,000 yr (21,000 yr) ago. These kinds of situations would have altered the location of the subsurface δ^{18}O peak as a result of changes in freshwater supply to the BoB area. Hence, modeling of the paleo-circulation may be constrained using the δ^{18}O-salinity regression coefficients determined in this study.

[27] **Acknowledgments.** The Indian Institute of Tropical Meteorology, Pune (IITM), is fully supported by Earth System Science Organization (ESSO) of Ministry of Earth Sciences, India. The authors also acknowledge the Department of Science and Technology for the project "Oceanographic Observations in the northern Bay of Bengal." Free software Ferret and GrADS are used in this study. We thank Satheesh Deekshith for technical assistance. Director, IITM, India, is acknowledged for his constant encouragement and scientific discussion. We thank M. Dileep Kumar and two anonymous reviewers for their critical comments which have improved the quality of the manuscript.

References

Abrahamsen, E. P., M. P. Meredith, K. K. Falkner, S. Torres-Valdes, M. J. Leng, M. B. Alkire, S. Bacon, S. W. Laxon, I. Polyakov, and V. Ivanov (2009), Tracer derived freshwater composition of the Siberian continental shelf and slope following the extreme Arctic summer of 2007, *Geophys. Res. Lett.*, *36*, L07602, doi:10.1029/2009GL037341.

Achuthavarier, D., and V. Krishnamurthy (2011), Role of Indian and Pacific SST in Indian summer monsoon intraseasonal variability, *J. Clim.*, *24*, 2915–2930.

Achyuthan, H., R. D. Deshpande, M. S. Rao, B. Kumar, T. Nallathambi, K. Shashi Kumar, R. Ramesh, P. Ramachandran, A. S. Maurya, and S. K. Gupta (2013), Stable isotopes and salinity in the surface waters of the Bay of Bengal: Implications for water dynamics and palaeoclimate, *Mar. Chem.*, *149*, 51–62.

Adkins, J. F., K. McIntyre, and D. P. Schrag (2002), The salinity, temperature, and δ^{18} O of the glacial deep ocean, *Science*, *298*, 1769–1773.

Agarwal, N., R. Sharma, A. Parekh, S. Basu, A. Sarkar, and V. K. Agarwal (2012), Argo observations of barrier Layer in the tropical Indian Ocean, *Adv. Space Res.*, *50*, 642–654.

Ahmad, S. M., G. Anil Babu, V. M. Padmakumari, A. M. Dayal, B. S. Sukhija, and P. Nagabhushanam (2005), Sr, Nd isotopic evidence of terrigenous flux variations in the Bay of Bengal: Implications of monsoons during the last ~34,000 years, *Geophys. Res. Lett.*, *32*, L22711, 1–4.

Benway, H. M., and A. C. Mix (2004), Oxygen isotopes, upper ocean salinity, and precipitation sources in the eastern tropical Pacific, Earth Planet. *Sci. Lett.*, *224*, 493–507.

Bhat, G. S., et al. (2001), BOMEX: The Bay of Bengal monsoon experiment, *Bull. Am. Meteorol. Soc.*, *82*, 2217–2243.

Bigg, G. R., and E. J. Rohling (2000), An oxygen isotope data set for marine waters, *J. Geophys. Res.*, *105*, 8527–8535.

Burton, K. W., and D. Vance (2000), Glacial-interglacial variations in the neodymium isotope composition of seawater in the Bay of Bengal recorded by planktonic foraminifera, *Earth Planet. Sci. Lett.*, *176*, 425–441.

Clowes, A. J., and G. E. R. Deacon (1935), The deep-water circulation of the Indian Ocean, *Nature*, *136*, 936–938.

Cullen, J. L. (1981), Microfossil evidence for changing salinity patterns in the Bay of Bengal over the last 20,000 years, *Palaeogeogr. Palaeoclimatol. Palaeoecol.*, *35*, 315–356.

Delaygue, G., E. Bard, C. Rollion, J. Jouzel, M. Stievenard, J.-C. Duplessy, and G. Ganssen (2001), Oxygen isotope/salinity relationship in the northern Indian Ocean, *J. Geophys. Res.*, *106*, 4565–4574.

Duplessy, J. C. (1982), Glacial to interglacial contrasts in the northern Indian Ocean, *Nature*, *295*, 494–498.

Durand, F., D. Shankar, F. Birol, and S. S. C. Shenoi (2009), Spatio temporal structure of the East India Coastal Current from satellite altimetry, *J. Geophys. Res.*, *114*, C02013, doi:10.1029/2008JC004807.

Dutta, K., and R. Bhushan (2012), Radiocarbon in the Northern Indian Ocean two decades after GEOSECS, *Global Biogeochem. Cycles*, *26*, GB2018, doi:10.1029/2010GB004027.

Epstein, S., and T. Mayeda (1953), Variation of O18 content of water from natural sources, *Geochim. Cosmochim. Acta*, *4*, 213–224.

Fairbanks, R. G. (1982), The origin of Continental Shelf and Slope Water in the New York Bight and Gulf of Maine evidence from $H_2{}^{18}O/H_2{}^{16}O$ ratio measurements, *J. Geophys. Res.*, *87*, 5796–5808.

Fofonoff, N. P., and R. C. Millard (1984), Algorithms for computation of fundamental properties of seawater, *Unesco Tech. Pap. in Mar. Sci. 44*, Paris, 53 pp.

Frew, R. D., K. Heywood, and P. F. Dennis (1995), Oxygen isotope study of water masses in the Princess Elizabeth Trough, *Mar. Chem.*, *49*, 141–153.

Frew, R. D., P. F. Dennis, K. J. Heywood, M. P. Meredith, and S. M. Boswell (2000), The oxygen isotope composition of water masses in the northern North Atlantic, *Deep Sea Res., Part I*, *47*(12), 2265–2286.

Girishkumar, M. S., M. Ravichandran, M. J. McPhaden, and R. R. Rao (2011), Intraseasonal variability in barrier layer thickness in the south central Bay of Bengal, *J. Geophys. Res.*, *116*, C03009, doi:10.1029/2010JC006657.

Gopalakrishna, V. V., V. S. N. Murty, D. Sengupta, S. Shenoy, and N. Araligidad (2002), Upper ocean stratification and circulation in the northern Bay of Bengal during the southwest monsoon of 1991, *Cont. Shelf Res.*, *22*, 791–802.

Hirst, A. C., and W. Cai (1994), Sensitivity of a world ocean GCM to changes in subsurface mixing parameterization, *J. Phys. Oceanogr.*, *24*, 1256–1279.

Klingaman, N. P., P. M. Inness, H. Weller, and J. M. Slingo (2008), The importance of high-frequency sea surface temperature variability to the intraseasonal oscillation of Indian monsoon rainfall, *J. Clim.*, *21*, 6119–6140.

Kumar, M. D., and Y.-H. Li (1996), Spreading of water masses and regeneration of 226Ra and Silica in the Indian Ocean, *Deep Sea Res., Part II*, *43*, 83–110.

LeGrande, A. N., and G. A. Schmidt (2006), Global gridded data set of the oxygen isotopic composition in seawater, *Geophys. Res. Lett.*, *33*, L12604, doi:10.1029/2006GL026011.

Meredith, M. P., K. E. Grose, E. L. McDonagh, K. J. Heywood, R. D. Frew, and P. F. Dennis (1999), Distribution of oxygen isotopes in the water masses of Drake Passage and the South Atlantic, *J. Geophys. Res.*, *104*C9, 20,949–20,962, doi:10.1029/98JC02544.

Meredith, M. P., H. J. Venables, A. Clarke, H. W. Ducklow, M. Erickson, M. J. Leng, J. T. M. Lenaerts, and M. R. van den Broeke (2013), The freshwater system west of the Antarctic Peninsula: Spatial and temporal changes, *J. Clim.*, *26*, 1669–1684.

Murty, V. S. N., Y. V. B. Sarma, D. P. Rao, and C. S. Murty, (1992), Water characteristics, mixing and circulation in the Bay of Bengal during southwest monsoon, *J. Mar. Res.*, *50*, 207–228.

Murty, V. S. N., A. Suryanarayana, and D. P. Rao (1993), Current structure and volume transport across 12N in the Bay of Bengal, *Ind. J. Mar. Sci.*, *22*, 12–16.

Nakayama, N., Y. Yamanaka, and T. Gamo (2008), O2 consumption rate and its isotopic fractionation factor in the deep water of the Philippine Sea, *J. Oceanogr.*, *64*(3), 451–457, doi:10.1007/s10872-008-0038-9.

Naqvi, S. W. A., D. A. Jayakumar, M. Nair, M. D. Kumar, and M. D. George (1994), Nitrous oxide in the western Bay of Bengal, *Mar. Chem.*, *47*, 269–278.

Nyadjro, E. S., B. Subrahmanyam, V. S. N. Murty, and J. F. Shriver (2010), Salt transport in the near surface layer in the monsoon influenced Indian Ocean using HYCOM, *Geophys. Res. Lett.*, *37*, L15603, doi:10.1029/2010GL044127.

Ostlund, H. G., H. Craig, W. S. Broecker, and D. Spenser (1987), GEOSECS Atlantic, Pacific and Indian Ocean expeditions: Shorebased data and graphics, vol. 7, *Tech. Rep.*, Natl. Sci. Found., Wash., D. C.

Parekh, A., A. Sarkar, S. Shah, and M. S. Narayanan (2004), Low period variability in TMI measured SST over the Bay of Bengal during summer monsoon, *Curr. Sci.*, *87*, 791–796.

Pfirman, S., W. Haxby, H. Eicken, M. Jeffries, and D. Bauch (2004), Drifting Arctic sea ice archives changes in ocean surface conditions, *Geophys. Res. Lett.*, *31*, L19401, doi:10.1029/2004GL020666.

Pierson-Wickmann, A. C., L. Reisberg, C. France-Lanord, and H. R. Kudrass (2001), Os-Sr-Nd results from sediments in the Bay of Bengal: Implications for sediment transport and the marine Os record, *Paleoceanography*, *16*, 435–444.

Potemra, J. T. (2005), Indonesian throughflow transport variability estimated from satellite altimetry, *Oceanography*, *18*, 94–103.

Prasad, T. G. (2004), A comparison of mixed-layer dynamics between the Arabian Sea and Bay of Bengal: One-dimensional model results, *J. Geophys. Res.*, *109*, C03035, doi:10.1029/2003JC002000.

Rao, R. R., and R. Sivakumar (2003), Seasonal variability of sea surface salinity and salt budget of the mixed layer of the north Indian Ocean, *J. Geophys. Res.*, *108*(C1), 3009, doi:10.1029/2001JC000907.

Rao, S. A., et al. (2011), Modulation of SST, SSS over northern Bay of Bengal on ISO time scale, *J. Geophys. Res.*, *116*, C09026, doi:10.1029/2010JC006804.

Rashid, H., E. England, L. Thompson, and L. Polyak (2011), Late glacial to Holocene Indian summer monsoon variability based upon sediment records taken from the Bay of Bengal, *Terr. Atmos. Oceanic Sci.*, *22*(2), 215–228.

Ravichandran, M., D. Behringer, S. Siva Reddy, M. S. Girishkumar, N. Chacko, and R. Harikumar (2011), INCOIS-GODAS-MOM: Ocean analysis for the Indian Ocean: Configuration, validation and product dissemination, *INCOIS Tech. Rep., INCOIS-MOG-TR-2011-06*. Hyderabad.

Ravichandran, M., D. Behringer, S. Sivareddy, M. S. Girishkumar, N. Chacko, and R. Harikumar (2013), Evaluation of the global ocean data assimilation system at INCOIS: The tropical Indian ocean, *Ocean Modell.*, *69*, 123–135.

Sarkar, A., R. Ramesh, S. K. Bhattacharya, and G. Rajagopalan (1990), Oxygen isotope evidence for a stronger winter monsoon current during the last glaciations, *Nature*, *343*, 549–551.

Sarma, V. V. S. S. (2002), An evaluation of physical and biogeochemical processes regulating the oxygen minimum zone in the water column of the Bay of Bengal, *Global Biogeochem. Cycle*, *16*(4), 1099, doi:10.1029/2002GB001920.

Schott, F., and McCreary, J. P., Jr. (2001), The monsoon circulation of the Indian Ocean, *Prog. Oceanogr.*, *51*(1), 1–123, doi:10.1016/S0079-6611(01)00083-0.

Sengupta, D., P. K. Ray, and G. S. Bhat (2002), Spring warming of the Eastern Arabian Sea and Bay of Bengal from Buoy Data, *Geophys. Res. Lett.*, *29*(15), 1734, doi:10.1029/2002GL015340.

Sengupta, D., G. N. Bharath Raj, and S. S. C. Shenoi (2006), Surface freshwater from Bay of Bengal runoff and Indonesian Throughflow in the tropical Indian Ocean, *Geophys. Res. Lett.*, *33*, L22609, doi:10.1029/2006GL027573.

Shankar, D., P. N. Vinayachandran, and A. S. Unnikrishnan (2002), The monsoon currents in the north Indian Ocean, *Prog. Oceanogr.*, *52*, 63–120.

Shenoi, S. S. C., D. Shankar, and S. R. Shetye (2002), Differences in heat budgets of the near-surface Arabian Sea and Bay of Bengal: Implications for the summer monsoon, *J. Geophys. Res.*, *107*(C6), 3052, doi:10.1029/2000JC000679.

Shetye, S. R., A. D. Gouveia, D. Shankar, S. S. C. Shenoi, P. N. Vinayachandran, D. Sundar, G. S. Michael, and G. Nampoothiri (1996), Hydrography and circulation in the western Bay of Bengal during the northeast monsoon, *J. Geophys. Res.*, *101*, 14,011–14,025.

Singh, A., R. A. Jani, and R. Ramesh (2010), Spatiotemporal variations of the δ18O–salinity relation in the northern Indian Ocean, *Deep Sea Res., Part I*, *57*, 1422–1431.

Somayajulu, B. L. K., R. Rengarajan, and R. A. Jani (2002), Geochemical cycling in the Hooghly estuary, India, *Mar. Chem.*, *79*, 171–183.

Srivastava, R., R. Ramesh, S. Prakash, N. Anilkumar, and M. Sudhakar (2007), Oxygen isotope and salinity variations in the Indian sector of the Southern Ocean, *Geophys. Res. Lett.*, *34*, L24603, doi:10.1029/2007GL031790.

Thadathil, P., P. M. Muraleedharan, R. R. Rao, Y. K. Somayajulu, G. V. Reddy, and C. Revichandran (2007), Observed seasonal variability of barrier layer in the Bay of Bengal, *J. Geophys. Res.*, *112*, C02009, doi:10.1029/2006JC003651.

Tiwari, M., S. S. Nagoji, T. Kartik, G. Drishya, R. K. Parvathy, and S. Rajan (2013), Oxygen isotope–salinity relationships of discrete oceanic regions from India to Antarctica vis-à-vis surface hydrological processes, *J. Mar. Syst.*, *113–114*, 88–93.

Tomczak, M., and J. S. Godfrey (2003), *Regional Oceanography: An Introduction*, 2nd improved ed., p. 206, Daya Publ. House, Delhi.

Udaya Bhaskar, T. V. S., M. Ravichandran, and R. Devender (2007), An operational Objective analysis system at INCOIS for generation of Argo value Added products. Report No. INCOIS-MOG-ARGO-TR-04-2007, Indian National Centre for Ocean Information Services, Hyderabad, India.

van Aken, H. M., H. Ridderinkhof, and W. P. M. de Ruijter (2004), North Atlantic deep water in the south-western Indian Ocean, *Deep Sea Res., Part I*, *51*(6), 755–776.

Vinayachandran, P. N., Y. Masumoto, T. Mikawa, and T. Yamagata (1999), Intrusion of the southwest monsoon current into the Bay of Bengal, *J. Geophys. Res.*, *104*, 11,077–11,085.

Vinayachandran P. N., V. S. N. Murty, and V. Ramesh Babu (2002), Observations of barrier layer formation in the Bay of Bengal during summer monsoon, *J. Geophys. Res.*, *107*(C12), 8018, doi:10.1029/2001JC000831.

Vinayachandran, P. N., C. P. Neema, S. Mathew, and R. Remya (2012), Mechanisms of summer intraseasonal sea surface temperature oscillations in the Bay of Bengal, *J. Geophys. Res.*, *117*, C01005, doi:10.1029/2011JC007433.

Yi, Y., J. J. Gibson, L. W. Cooper, J.-F. Helie, S. J. Birks, J. W. McClelland, R. M. Holmes, and B. J. Peterson (2012), Isotopic signals (18O, 2H, 3H) of six major rivers draining the pan-Arctic watershed, *Global Biogeochem. Cycles*, *26*, GB1027 doi:10.1029/2011GB004159.